



COB-2021-1044

DESIGN AND CHARACTERIZATION OF A COMPACT ACTUATOR COMPOSED BY SMA MICRO-SPRINGS

José Fernando de Moraes Firmino
Cícero da Rocha Souto

Universidade Federal da Paraíba — UFPB, Campus I. Via Expressa Padre Zé, 499. Castelo Branco. João Pessoa-PB, 58050-425.
fernandodemorais.jf@gmail.com
cicerosouto@cear.ufpb.br

André Fellipe Cavalcante Silva

Instituto Federal da Paraíba — IFPB, Campus João Pessoa. Av. Primeiro de Maio, 720. Jaguaribe. João Pessoa-PB, 58015-435.
andre.cavalcante@ifpb.edu.br

Abstract. *In this paper it is presented the development and characterization of a movement mechanism composed by M12 shape memory alloy micro-springs, for application purposes in rehabilitation engineering field. It was designed to allow the movements of a given robotic finger, using two antagonistic pairs of SMA springs. This device was characterized in terms of maximum force, operation temperature and displacement. Was used, to characterize the force, a fixed load cell, type K thermocouples and a thin polyamide wire to connect the mechanism to the transducer. A webcam, in conjunction with the same thermocouples, was used to capture images of the free movement produced by the mechanism and such captures were processed by an algorithm, which determined the generated displacements. The obtained results demonstrate that the conceived mechanism was able to generate, approximately, 1.48 N of force, 99.6° of angular and 13.9 mm of linear displacement, reaching a temperature of 58.53 °C with its activation. Considering those results, an encouraging path can be observed for the application of the developed device in upper limbs bioinspired prototypes, since this kind of apparatus demand small actuators capable to describe good angular displacement and generate moderate forces.*

Keywords: *compact actuators, SMA micro-springs, experimental characterization, rehabilitation engineering.*

1. INTRODUCTION

Shape memory alloys, or SMA, are metallic alloys that have the ability to develop and recover considerable levels of deformation, with virtually no residual one. They are also able to generate significant force, by restricting their recovery, simply promoting their heating or the imposition of stresses, which causes phase transformations induced in the material (Emiliavaca, 2016; Silva, 2015).

One of the most popular SMA is the alloy formed by Nickel-Titanium, also known as nitinol (NiTi), capable of recovering deformations of up to 8%, characterizing them as susceptible to high performance applications. In addition, they are suitable for large forces generation, also possessing considerable mechanical strength and high damping capacity. By presenting such properties and performance characteristics, this family of materials was the best developed in recent decades (Emiliavaca, 2016).

According to Mohd Jani *et al.* (2014), research in the area showed that SMA actuators are excellent replacements for conventional ones, such as pneumatic, hydraulic and electric motors, due to its characteristics explained above. This implies the possibility of developing cheaper and more advanced actuation devices, in addition to being less complex, maintaining high density rates of work, being also, in the case of NiTi, biocompatible.

The use of SMA as non-conventional biomimetic prototype actuators has been continuously studied in recent years. In this group, robotic prostheses, or prosthetic devices, are highlighted, since, according to Pons (2008), they are electromechanical apparatus specially designed to replace, by means of a wearable robotic limb, the lost human counterpart as close as possible to its original functions.

Adding to the author's definition, beyond the functions of the lost limb, robotic devices with prosthetic purposes can also be designed in order to respect, as much as possible, the anthropomorphic aspects of their human counterpart, seeking to generate greater comfort for the user, in which it concerns its daily use in front of other people. These are, thus, biomimetic devices, as they aim at both the functional and aesthetic replacement of the limb.

In that regard, the purpose of this work was to develop and characterize an actuation device composed of two pairs of NiTi SMA micro-springs, in an antagonistic disposition, capable of performing angular displacements appropriate to the movement of the phalanges of a given robotic finger, in replacement of conventional actuators.

2. MATERIALS AND METHODS

This research was developed in two distinct, however complementary, stages. The first one, the development of the actuation mechanism, concentrates the application of the study carried out on actuators composed of shape memory alloys, their behavior and the methodology for taking advantage of their properties.

The development of the first stage took place with the selection of the most suitable actuator for the application, the design and prototyping of its mechanical structure, the elaboration of the drive circuit and, finally, its characterization.

The second stage consisted of data processing, obtained with the characterization, aiming to quantify the force and displacement generation capabilities of the developed mechanism.

2.1 Mechanical structure

For the design of the mechanical structure of the phalanges actuation device, a research related to SMA materials was necessary, whose characteristics allowed the use of their capabilities (the generation of force and displacement with its activation) within a compact structure.

In that regard, taking into account the purpose of the application, the studies carried out by Basilio Sobrinho *et al.* (2017) and Emiliavaca (2016), who not only performed a thermomechanical characterization of the materials, but also designed structures and application methods, guided the selection of NiTi SMA M12 helical micro-springs as actuators of the designed mechanism.

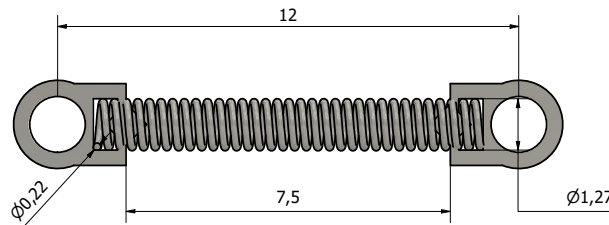


Figure 1. Dimensions, in mm, common to the M12 micro-springs used.

As can be seen in Fig. 1, these closed springs, commercially available and for orthodontic application, have 12 mm between the centers of the bezel eyelets. However, its usable length is 7.5 mm. They also have, on average, 27 active coils, 1.27 mm of spring diameter and 0.22 mm (220 μm) of wire diameter, which characterizes them as micro-springs (Emiliavaca, 2016).

One of the main factors that influenced the selection of these materials as actuators is its reduced dimensions, summed with the ability to deform, when subjected to a constant mechanical loading (forming stress-induced martensite), reversibly, up to 600% of its initial length. This characteristic allows them to compose compact structures and devices with reduced mass (Basilio Sobrinho *et al.*, 2017). Furthermore, if subjected to a heating higher than the final austenite temperature (with a new phase transformation occurring, returning to the austenite phase), they are able to generate force and perform work. In this way, it is possible to recover almost all of the initial deformation under load (Emiliavaca, 2016).

Many studies in the field of rehabilitation engineering that involved the elaboration of actuators composed of SMA materials, used them in NiTi thin wire forms. A perceived disadvantage in this practice is the fact that, for the generation of significant displacement, long wire lengths are needed and, therefore, mechanical arrangements to condense this required volume are essential, as can be seen in the works of Silva (2015) and Andrianesis and Tzes (2015). According to Emiliavaca *et al.* (2019), the level of fully recoverable linear deformation of these wires is at 5%.

According to the results of the tensile test carried out by Basilio Sobrinho *et al.* (2017), the equilibrium point of these springs, the point where the phase transformation to final deformation-induced martensite occurs, is found at about 350% of elongation, approximately 38.25 mm long. The determination of this parameter was essential to identify the attachment points of the actuators on the mechanism, enabling, as stated by Silva *et al.* (2017), to maximize the shape memory effect, according to the combination of the initial deformation (350%), the maximum (approximately 400% of deformation) and the minimum (approximately 300% of elongation) of the micro-springs inserted in the designed device. Therefore, keeping in mind the characteristics mentioned above, a mechanism was conceived that includes the elements illustrated in Fig. 2.

The device was designed to allow the independent actuation of each pair of springs, so they can execute circular movements in opposite directions. When the pair of micro-springs on the front, following the perspective presented in Fig. 3 a), when heated (by the Joule effect, in this work) recovers its deformation, movement will be generated in the counterclockwise direction, while the pair at the rear will be further elongated. By contrast, illustrated in Fig. 3 b), when heating the pair at the rear of the mechanism, motion will be generated in the clockwise direction and, consequently, the front pair will deform even more.

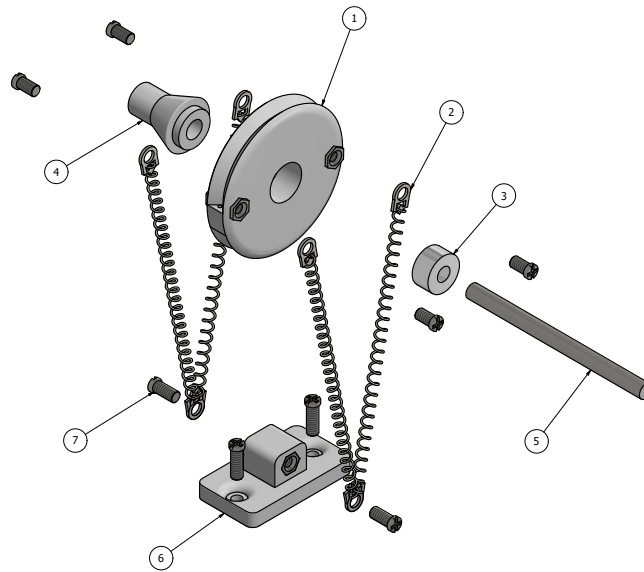


Figure 2. Exploded view of the designed actuation mechanism. Where: 1. ABS pulley with $\varnothing 18$ mm and four M1.4 nuts, embedded in its structure; 2. M12 SMA micro-springs; 3. MR 52 ZZ micro bearing; 4. ABS spacer; 5. steel shaft with $\varnothing 2$ mm; 6. ABS anchor with two M1.4 nuts embedded; and 7. M1.4 screws.

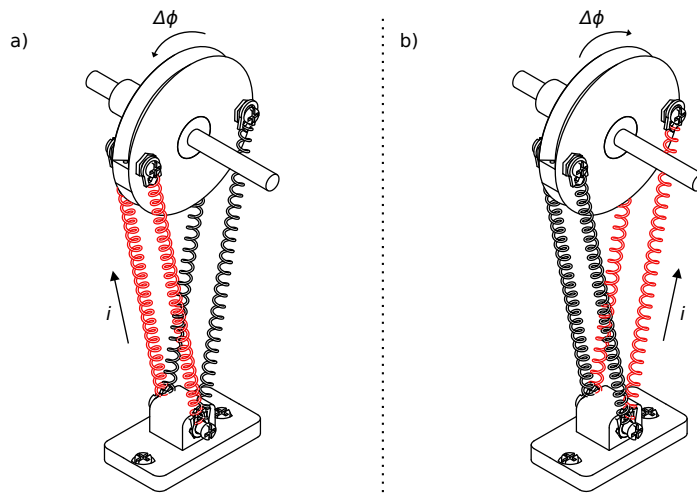


Figure 3. Representation of the movements performed by the mechanism. Where: a) from intermediate position to counterclockwise movement; and b) from intermediate position to clockwise movement.

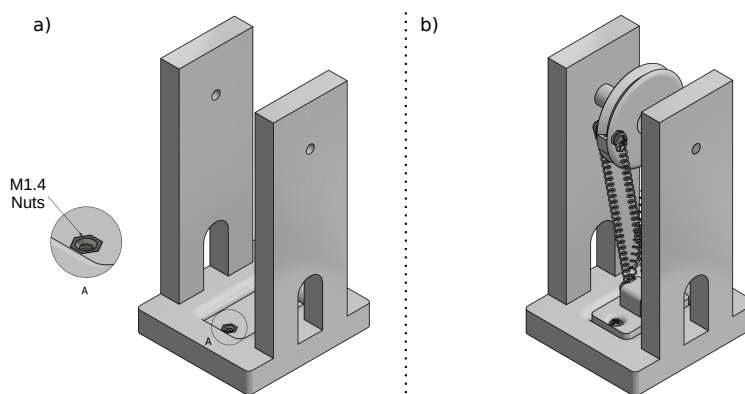


Figure 4. Actuation mechanism assembled in a base. Where: a) mechanism base, in ABS, with two M1.4 nuts for fixing the anchor; and b) mechanism assembled in the base.

These movements described above are fundamental for the activation of a robotic finger, since its phalanges must perform flexion and extension movements, which correspond to those produced by the designed actuation mechanism.

In order to facilitate the assembly of the mechanism and enable its characterization, an ABS base was created. Such a base can be seen in Fig. 4. It is worth emphasizing, that in the pulley of the designed device, there are small regions to tie thin polyamide wires (more precisely $\varnothing 0.3$ mm), which are responsible for transmitting the movement generated by the activation of the SMA micro-springs.

2.2 Activation

For the purpose of triggering the actuators, using the method of heating by the Joule effect, a current source circuit, controlled by input voltage, was designed, using operational amplifiers and bipolar transistors, as well as the Arduino Nano open microcontroller platform, which enabled a level of automation in the activation of the micro-springs and in the acquisition of signals during the characterization of the mechanism.

It was necessary to perform, in the drive circuit of the device developed in this work, an arrangement in the conventional topology of the mentioned source to generate a signal amplification, so that there was a direct conversion of the electric voltage value at the input into current at the output.

To ensure that the electrical voltage signal at the input was the desired, the MCP4725 digital-analog converter module, connected to an Arduino Nano through the I²C bus, was used. The circuit is supplied with 12 V that pass through a LM2596 step-down voltage regulator, whose output, adjusted at 5 V, feeds the digital-analog converter module and a LM324 IC (operational amplifiers).

The SMA micro-springs, on the other hand, are powered directly by the current source, and each pair (connected in series with the source output) is activated intermittently when polarizing a Darlington TIP122 transistor, whose bases are each connected to an Arduino Nano digital pin. So, in this way, by providing an input signal to the source and changing the state of the corresponding microcontroller pin, it is possible to trigger the pair responsible for performing the desired movement.

The maximum current generated at the source output, for a single pair of springs connected in series, is approximately 640 mA. This value of maximum generated current is more than enough to heat, through the Joule effect, the actuators to the final austenite temperature, with a value of 0.4 A being the most common for this purpose, as seen in the works of Silva *et al.* (2017) and Emiliavaca *et al.* (2019).

2.3 Characterization

For the proper characterization of the device, two different methodologies were developed: one to determine the maximum force and another to measure the displacement, both generated with the activation of the elaborated mechanism. These two capabilities are essential for an assertive application of the device.

Therefore, for the characterization of the force generated by the activation of the mechanism, an experimental workbench was created, and that included, in addition to the designed circuit, a 1 kg load cell, a programmable HX711 amplification module (for use with the cell), a type K thermocouple and a MAX6675 signal digitizer.

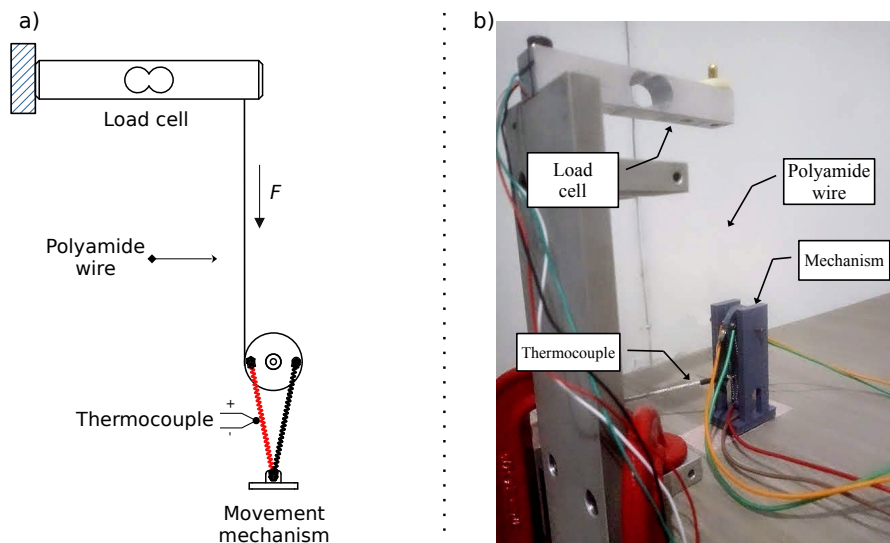


Figure 5. Experimental workbench for the characterization of the generated force. Where: a) layout; and b) photo of the assembled workbench.

In Fig. 5 can be seeing the elements that compose the experimental workbench properly assembled. As indicated in the image, there is a thin polyamide wire, with $\varnothing 0.3$ mm, connecting the movement mechanism pulley to the load cell used. Because it is transparent, has a reduced diameter and also the distance necessary to frame all the elements in the image, it is not possible to view it.

With the use of the experimental workbench, acquisitions of 800 points of force were carried out at a frequency of 10 Hz. At the same time, 400 temperature readings of the activated SMA micro-spring were acquired, these at 5 Hz due to the hardware limitations of the MAX6675 module, and it was necessary, after the process, to promote the interpolation of these data according to the parameters of force acquisition, to facilitate the analyses. It is noteworthy that another type K thermocouple (and consequently another digitizer module) was used to measure the room temperature, allowing comparisons between them. In addition, the load cell was properly calibrated before carrying out the experiment.

As for the measurement of the angular and linear displacement produced by the mechanism, the image processing methodology was used, aiming to ensure greater reliability in the acquisition of the movement data performed. In this way, practically the same instrumentation hardware used in the previous experiment was reused, with only the load cell and the HX711 module having been replaced (thereby keeping, in addition to the drive circuit, the type K thermocouples and the MAX6675 modules) by a conventional webcam, with typical image generation at 480p resolution (640 × 480 pixels).

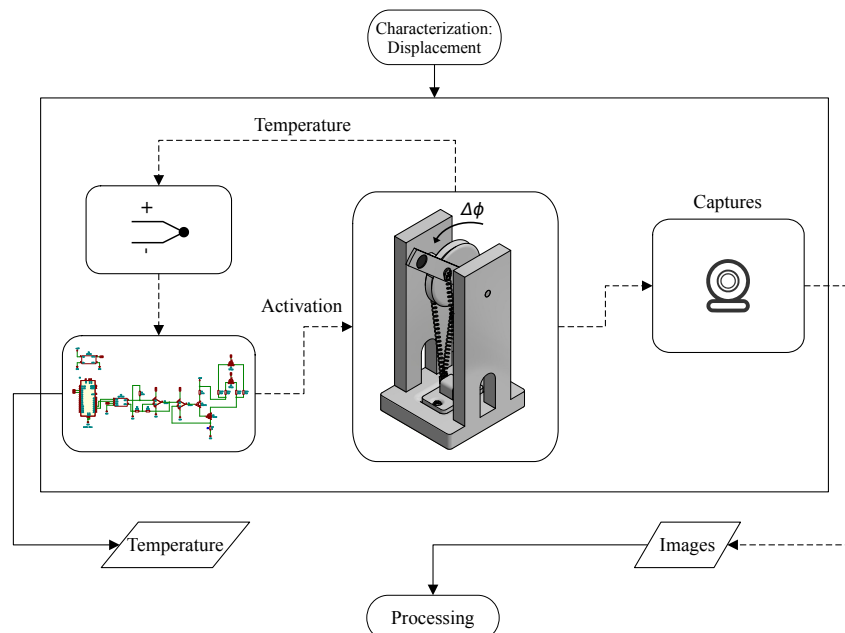


Figure 6. Layout of the experimental workbench for the characterization of the generated displacement.

Observing the Fig. 6, it is possible to notice the addition of an extender centered on the pulley of the actuation mechanism. It has been specially designed so that, when screwed onto the mechanical component, the distance between the center of the shaft and the center of the point marked on it is known.

To characterize the displacement mechanism, two algorithms were developed in the Python language: one capable of receiving an image as input, filtering it and processing it to the point of contouring regions of interest, identifying the coordinates of their centers and returning them along with its distance (in pixels) to the user; and another to control the webcam, so that it would be possible to capture images at a certain acquisition frequency.

It is noteworthy that the experiment was carried out by activating the mechanism from its maximum point of extension to its maximum point of flexion, considering the types of movements performed by the phalanges of the human finger. In other words: it started from the point where the pair of micro-springs responsible for the clockwise movement direction (according to the perspective presented in Fig. 6) was at its maximum recovery point, followed by the activation of the pair that generates counterclockwise movement, until it reached its maximum recovery.

Therewith, 800 image captures were performed, at an acquisition frequency of 10 Hz. Along with them, temperature readings were taken using the type K thermocouple and the MAX6675 module, following the same method used in the force characterization, making it possible to determine the angular position of the mechanism pulley throughout the described movement and calculate the angular and linear displacement, considering, for these calculations, respectively, the distance between the center of the shaft of the device and the center of the mark on the attached extender (larger radius), as well as the distance between the center of the pulley and the bezel area for the polyamide wires.

3. RESULTS AND DISCUSSIONS

With the application of the detailed methodology, for the characterization of the mechanism developed by means of rapid prototyping, a set of data related to the intrinsic characteristics of this device was obtained, regarding the force and the linear and angular displacement generated with its activation.

3.1 Force

The experiment was carried out to characterize the force generated by the activation of the mechanism, which involved the setting of a thin polyamide wire between the pulley present in the device and the 1 kg load cell used (as represented in the Fig. 5), as well as the use of type K thermocouples to read the room temperature and to which the SMA micro-spring was subjected during the test, thus, data were obtained that made it possible to relate: the force as a function of the activation time; temperature as a function of time; and force as a function of temperature.

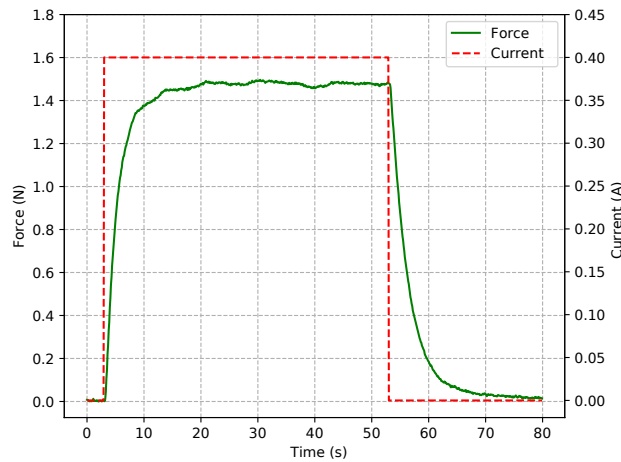


Figure 7. Graph of Force and Current vs. Time.

The result presented in Fig. 7 demonstrates that the maximum force reached by the activation of the mechanism was, approximately, 1.48 N, in the application of an electric current step of 0.4 A. The time required for the pair of actuators to reach its maximum point was around 21 s (considering the total acquisition time), or 18 s, excluding the first three seconds of inactivity.

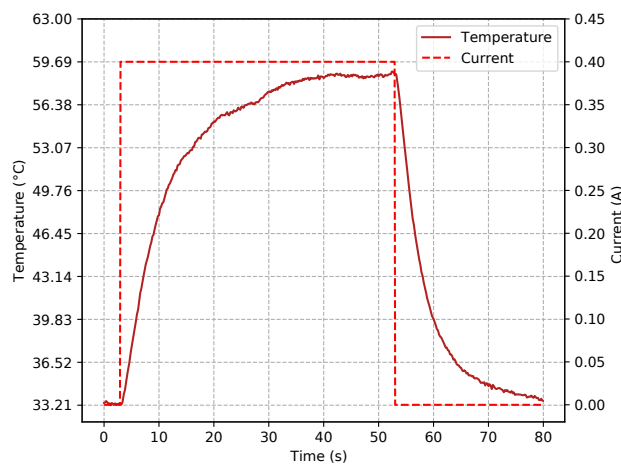


Figure 8. Graph of Temperature and Current vs. Time

As seen in Fig. 8, when a step of 0.4 A was applied, the actuator had a maximum temperature of 58.5 °C, approximately, activated at room temperature, which was in 33.2 °C. The approximate time required for this was 43 s (or 40 s, if the first three seconds of inactivity are disregarded). As already mentioned, two type K thermocouples were used to perform the temperature readings: one for the actuator and the other for the room.

The results shown above are consistent with the use of these actuators in compact structures, whose equilibrium point of application is at 350% of elongation. This can be validated in the information presented in studies in related areas, such

as the one elaborated by Basilio Sobrinho *et al.* (2020) who arranged the M12 SMA micro-springs in a small motor, in addition to characterizing the device numerically and experimentally. The values presented by them are similar to those described here.

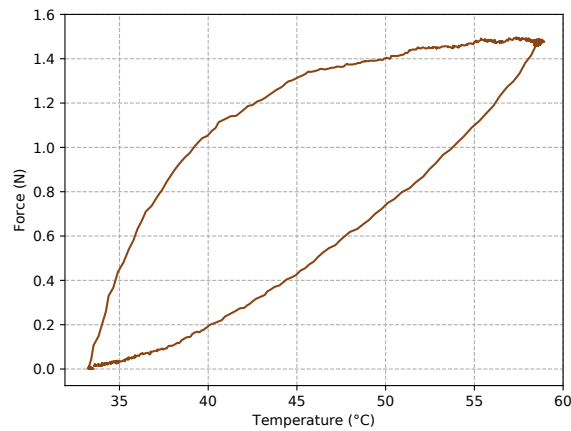


Figure 9. Graph of Force vs. Temperature.

With the data obtained, it was feasible to relate the force generated with the temperature reached, aiming a visual analysis of the quantization of these quantities during the test. The Fig. 9 graph shows the hysteretic behavior of the material, and this information is of great importance to be considered in the development of control structures, or even for drives and other applications of the mechanism developed and characterized in this work.

3.2 Displacement

The experiment was carried out to characterize the displacement (angular and linear) generated by the activation of the device, which involved, as shown in the Fig. 6, the fixation of an extender on the pulley of the mechanism, the use of type K thermocouples (under the same conditions as the previous test) and a webcam for image captures, therefore data were obtained that enabled the relationship between: the described angle and the activation time; the angle and temperature of the actuator; displacement and time; and displacement and temperature.

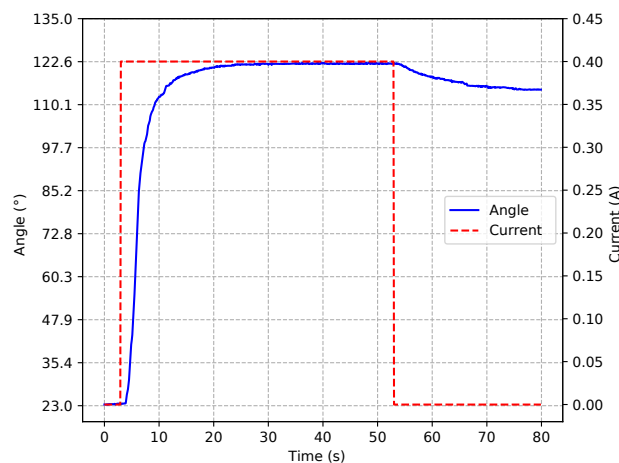


Figure 10. Graph of Angle and Current vs. Time.

Observing the graph in Fig. 10, it can be seen that the maximum angulation reached with the movement was 122.6°, applying an electrical current step of 0.4 A. The time required for this was approximately 24 s. However, when disregarding the first three, it took 21 s for the mechanism to complete its movement. It is also possible to note that the maximum extension point (movement performed by the actuator in a clockwise direction, considering the perspective presented in Fig. 6), was at 23°, which is the starting point of the pulley in this test. The angular variation, or angular displacement ($\Delta\phi$), obtained was 99.6°.

As can be seen in the graphic of Fig. 10, it is noticed in the Fig. 11 that after the current supply ceases and, consequently, the actuator cools down, the force imposed by the pair of antagonistic springs caused the pulley to recoil about 9° in the direction of the extension movement.

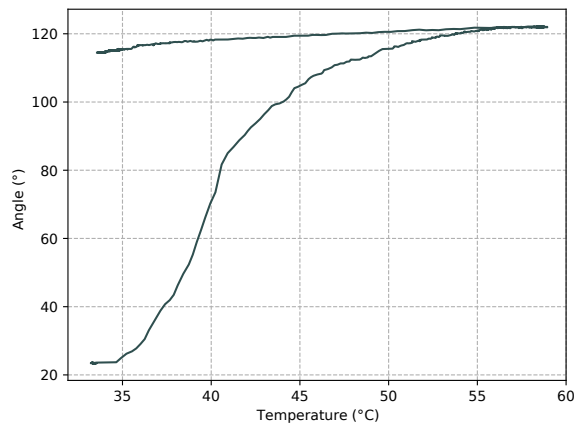


Figure 11. Graph of Angle vs. Temperature.

From the results presented in the last two graphs, the relations and properties of the circular movement and the transmission of movements were used to determine the linear displacement (ΔS) promoted by the activation of the mechanism.

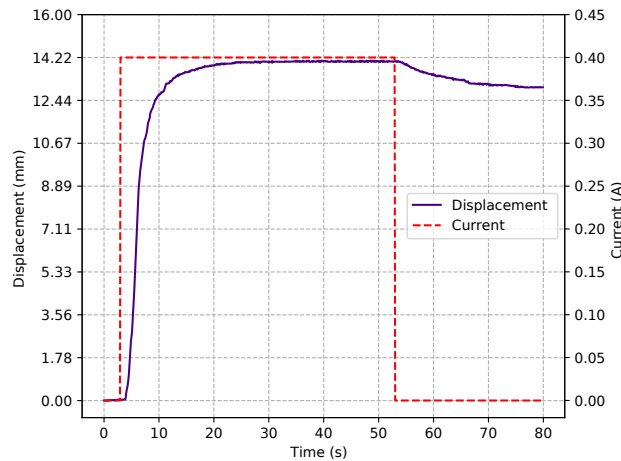


Figure 12. Displacement and Current vs. Time.

To calculate the results presented in the Fig. 12, the total $\Delta\phi$, of 99.6° , and the distance between the center of the pulley to the location for setting the polyamide wire in it, whose value is 8 mm, was used. With this, a ΔS of approximately 13.9 mm was obtained. Analogous to that represented in Fig. 10, the time needed to form this arc was 21 s, excluding the first three seconds of inactivity.

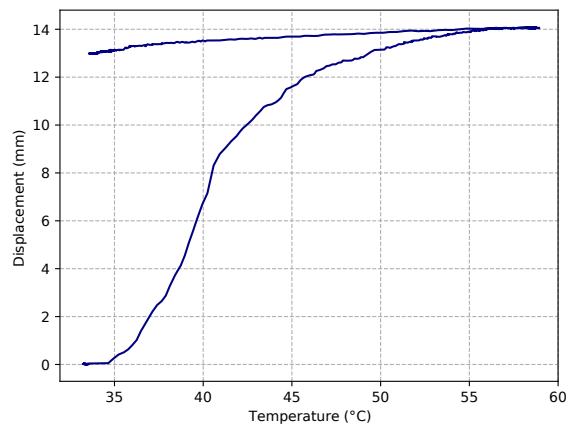


Figure 13. Graph of Displacement vs. Temperature.

Figure 13 contains the graph that relates the displacement generated with the temperature reached by triggering the actuators and, similarly to the one presented in Fig. 11, with cooling, there was a recoil of about 1 mm imposed by the force of the antagonistic pair of springs.

4. CONCLUSIONS

The results obtained with the movement characterization of the developed mechanism proved to be very encouraging, considering its application in the field of rehabilitation engineering, since active robotic prostheses for upper limbs need a successful use of mechanical arrangements capable of perform significant displacements, such as those presented.

As can be seen in the medical literature (Levangie and Norkin, 2011), the angular displacement generated with the activation of the mechanism's micro-springs (99.6°) is sufficient to move the phalanges of an adult human finger to the typical angulations formed with its flexion, because: a proximal phalanx forms, on average, an angle of 90° ; the medial forms a minimum of 100° ; and the distal, 80° .

The device developed proved to be compact enough for applications in the field of rehabilitation engineering, in addition to enabling a wider range of use, given the amount of force and displacements, angular and linear, generated with its activation. Therefore, it is expected that this study will contribute to the development of further advances in the application of shape memory alloy materials (as well as the movement mechanism detailed here) for the development of robotic devices, including active prostheses.

5. ACKNOWLEDGEMENTS

This study was financed in part by the Coordenação de Aperfeiçoamento de Pessoal de Nível Superior - Brasil (CAPES) - Finance Code 001.

6. REFERENCES

- Andrianesis, K. and Tzes, A., 2015. "Development and Control of a Multifunctional Prosthetic Hand with Shape Memory Alloy Actuators". *Journal of Intelligent & Robotic Systems*, Vol. 78, No. 2, pp. 257–289. ISSN 1573-0409. doi: 10.1007/s10846-014-0061-6.
- Basilio Sobrinho, J.M., Filho, F.M.F., Emiliavaca, A., Cunha, M.F., Souto, C.R., Silva, S.A. and Ries, A., 2020. "Experimental and numerical analyses of a rotary motor using shape memory alloy mini springs". *Sensors and Actuators A: Physical*, Vol. 302, pp. 1–12. ISSN 0924-4247. doi:10.1016/j.sna.2019.111823.
- Basilio Sobrinho, J.M., Cunha, M.F., Souto, C.d.R., da Silva, S.A., dos Santos, A.J.V. and Catunda, S.Y.C., 2017. "Electronic instrumentation for the characterization of a rotary thermoelectric motor driven by shape memory alloy springs". In *2017 IEEE International Instrumentation and Measurement Technology Conference (I2MTC)*. IEEE, Turim, Itália, pp. 1–5. ISBN 978-1-5090-3596-0. doi:10.1109/I2MTC.2017.7969933.
- Emiliavaca, A., 2016. *SMARt MORPHING WING: um protótipo de asa adaptativa acionada por micromolas de liga com memória de forma*. Master's thesis, Federal University of Campina Grande, Campina Grande. Mechanical Engineering Course.
- Emiliavaca, A., de Araújo, C.J., Souto, C.d.R. and Ries, A., 2019. "Characterization of shape memory alloy micro-springs for application in morphing wings". *Smart Materials and Structures*, Vol. 28, No. 1, pp. 1–13. ISSN 0964-1726, 1361-665X. doi:10.1088/1361-665X/aaeb80.
- Levangie, P.K. and Norkin, C.C., 2011. *Joint Structure and Function: A Comprehensive Analysis*. F. A. Davis Company, Philadelphia, 5th edition. ISBN 978-0-8036-2362-0.
- Mohd Jani, J., Leary, M., Subic, A. and Gibson, M.A., 2014. "A review of shape memory alloy research, applications and opportunities". *Materials & Design (1980-2015)*, Vol. 56, pp. 1078–1113. ISSN 02613069. doi:10.1016/j.matdes.2013.11.084.
- Pons, J.L., ed., 2008. *Wearable Robots: Biomechatronic Exoskeletons*. John Wiley & Sons Ltd, Chichester, 1st edition. ISBN 978-0-470-51294-4.
- Silva, A.F.C., 2015. *Desenvolvimento e caracterização de uma mão robótica acionada por atuadores de liga com memória de forma*. Ph.D. thesis, Federal University of Paraíba, João Pessoa. Mechanical Engineering Course.
- Silva, A.F.C., Avelino, E.T.F., Nóbrega, A.M.d.S. and Firmino, J.F.d.M., 2017. "Dedo robótico acionado por molas de liga com memória de forma". *Revista Principia*, , No. 36, pp. 60–67. doi:10.18265/1517-03062015v1n36p60-67.

7. RESPONSIBILITY NOTICE

The authors are solely responsible for the printed material included in this paper.